Computational Mechanics 28 (2002) 331–338 © Springer-Verlag 2002
DOI 10.1007/s00466-001-0297-4

A study on time schemes for DRBEM analysis of elastic impact wave

W. Chen, M. Tanaka

Abstract The precise integration and differential quadrature methods are two new unconditionally stable numerical schemes to approximate time derivative with more than the second order accuracy. Recent studies showed that compared with the Houbolt and Newmark methods, they produced more accurate solutions with large time step for the problems where response is primarily dominated by low and intermediate frequency modes. This paper aims to investigate these time schemes in the context of the dual reciprocity BEM (DRBEM) formulation of various shock-excited scalar elastic wave problems, where high modes have important affect on traction response. The Houbolt method was widely recommended in many literatures for such DRBEM dynamic formulations. However, this study found that the damped Newmark algorithm was the most efficient and accurate for impact traction analysis in conjunction with the DRBEM. The precise integration and differential quadrature methods are shown inapplicable for such shock-excited problems due to the absence of numerical damping. On the other hand, we also found that to achieve the same order of accuracy, the differential quadrature method required much less computing effort than the precise integration method due to the use of the Bartels–Stewart algorithm solving the resulting Lyapunov matrix analogization equation.

Keywords Plates, Impact, Time integration, Boundary element method

1 Introduction

In recent years, the dual reciprocity BEM (DRBEM) has become increasingly popular in the numerical solution of various dynamic problems due to its intrinsic boundary-only merit and flexibility of applying fundamental solutions. The resulting DRBEM formulation of dynamic problems can be expressed in the standard form of ordinary differential equations of initial value problems and is therefore applicable to be solved by various mature time integrators (Nardini and Brebbia 1983; Partridge et al. 1992). The essence which distinguishes the DRBEM from other BEM techniques is to employ the radial basis function (Golberg et al. 1998; Chen and Tanaka 2000), which erases to a great extent the inefficiency of the normal BEMs handling inhomogeneous terms as in nonlinear and dynamic problems. It has been widely revealed that the DRBEM can approximate the spatial derivatives very accurately. Therefore, the accuracy, computing efficiency and stability of the DRBEM solutions of dynamic problems depend greatly on the proper choice of time-marching schemes (Loeffler and Mansur 1987; Partridge et al. 1992). For problems in which the response is dominated by the low and intermediate frequency components of the system, it was found that all implicit schemes produce the accurate solutions if time step is small enough. In particular, the differential quadrature method (DQM) was shown very efficient and accurate using coarse time step (Tanaka and Chen 2000).

However, it is a quite different situation for problems in which the contributions of high frequency modes to the response are important. To depress the influences of high modes, the numerical damping is in general required. The Houbolt method was often recommended due to its high artificial damping (Loeffler and Mansur 1987; Partridge et al. 1992; Kontoni and Beskos 1993). In particular, Agnantiaris et al. (1998) tested the DRBEM to 3D elastodynamic problems subject to the Heaviside-type impact. Only the displacement response results are displayed there. They claim that the Newmark and Wilson methods are not stable and accurate without giving supportive details and only the Houbolt method and Park's method (Park 1975) are applied and advocated. Theoretically, we could not find the advantages of the Houbolt method with the high artificial damping since the displacement responses in all these impact cases are still rather smooth. In other words, the high-frequency components do not have important effect on these displacement responses. Also through numerical experiments, Tanaka and Chen (2000) found that the Newmark method with the proper choice of its parameters outperformed well over the Houbolt method in the calculation of the displacement responses of the scalar bar subject to the Heaviside impact. On the other hand, Hilber and Hughes (1978) pointed out that the self-starting is one of essentially desirable properties of a competitive numerical integrator for dynamics problems,

Received 6 November 2000

W. Chen, M. Tanaka (✉)
Department of Mechanical Systems Engineering,
Shinshu University, Wakasato 4-17-1,
Nagano 380-8553, Japan
e-mail: dtanaka@gipwc.shinshu-u.ac.jp

This work was carried out as a part of the research program supported by the Japan Society for Promotion of Science. Additional financial support was provided by the Monbusho Grant-in-Aid. Some valuable comments from a referee reshaped this paper into its present form.

while the Houbolt method necessarily requires a distinct starting procedure and fails to satisfy this condition. The time integrators of such type not only increase the programming labor but also may cause some complexity of computing (Subbaraj and Dokainish 1989). Kogl and Gaul (1999) proposed an alternative Newmark scheme with significant numerical damping. A numerical experiment given there prefers to their damped Newmark method. It is noted that Agnantiaris et al. (1998) do not show the results of traction responses which in general have the solution of higher-order discontinuity. Namely, the numerical damping should be much more beneficial in the calculation of traction history than in that of the displacement history. In this study, both traction and displacement responses of elastic bar subject to various kinds of outer impact forces will be analysed in details with the Newmark and Houbolt methods.

The DQM can be considered as the "direct approach" of the traditional collocation (pseudo-spectral) methods in that the governing equations are analogized in terms of practical physical variables instead of usually fictitious expansion (spectral) coefficients (Bert and Malik 1996; Chen 1996). The advantages of the DQM over the latter lie in the ease of its implementation and more flexibility to choose grid points. The DQM has been extensively employed to approximate spatial partial derivative. The method can yield highly accurate solutions to the boundary value problems with a minimal computing effort, namely, so-called spectral accuracy (Bert and Malik 1996). The shortcoming of this method is the lack of geometry flexibility. It is noted that the time variable has the simplicity of geometry. The DQM analogue of the temporal derivative was demonstrated to perform very well in terms of accuracy, efficiency and stability (Chen 1996; Tanaka and Chen 2000, 2001). In particular, the DQM was found to be the only one efficient time scheme for solving the DRBEM formulation of transient diffusion problems with Dirichlet boundary conditions (Tanaka and Chen 2001).

On the other hand, Zhong and Williams (1994) presented a so-called precise integration method (PIM). The method is in fact equivalent to the exponential matrix approach as referred to in Turjillo (1997) and other literature. The merit of the PIM is that it uses a recurrence formula to reduce the computing effort and simplifies the use of the exponential matrix method. It was claimed that the method can produce highly precise solutions yet keeping unconditional stability for various dynamic problems (Lin et al. 1996). However, this method has not yet been tested to the elastodynamic impact problems.

The purpose of this paper is to evaluate performances of the DQM, PIM, Houbolt, and Newmark methods for elastodynamic impact–response problems in conjunction with the DRBEM space discretization. The numerical examples considered are the shock-excited in-plane plate vibration which is prone to severe numerical instability (Loeffler and Mansur 1987). The resulting DQM and DRBEM mixed formulation is found the known Lyapunov matrix equation. The Bartels–Stewart algorithm is used here to greatly reduce the computing effort in the solution of this Lyapunov matrix equation. It is worth stressing that all these four time integrators are unconditionally stable.

2 DRBEM discretization in space

The equation governing longitudinal vibration of damped plates can be expressed as

$$\nabla^2 u(x,t) = \frac{1}{\mu^2}\frac{\partial^2 u(x,t)}{\partial t^2} + \lambda \frac{\partial u(x,t)}{\partial t}, \quad x \in \Omega \ , \tag{1}$$

where λ is the coefficient of velocity-dependent external viscous damping. Note that the plain outer force is enforced through boundary as shown in Fig. 1. The initial conditions are

$$u(x,0) = u_0(x) \ , \tag{2a}$$

$$\dot{u}(x,0) = v_0(x) \ , \tag{2b}$$

and the displacement and traction boundary conditions are given by

$$u(x,t) = \bar{u}(x,t), \quad x \subset \Gamma_u \ , \tag{3}$$

$$T(x,t) = \bar{T}(x,t), \quad x \subset \Gamma_T \ , \tag{4}$$

where variable domain $\Omega \in R^2$ is bounded by a piece-wise smooth boundary $\Gamma = \Gamma_u + \Gamma_T$, and $T = \partial u/\partial n$, n is the unit outward normal.

The governing equation (1) can be weighted by the fundamental solution u^* of Laplace operator. By using Green's second identity, we have

$$d_i u_i + \int_\Gamma (T^* u - u^* T)\mathrm{d}\Gamma = -\int_\Omega \left(\frac{1}{\mu^2}\frac{\partial^2 u}{\partial t^2} + \lambda\frac{\partial u}{\partial t}\right) u^* \,\mathrm{d}\Omega \ , \tag{5}$$

where subscript i denotes the source point, $T^* = \partial u^*/\partial n$, and $d_i = \int_\Omega \delta(\zeta, x)\mathrm{d}\Omega$. The dual reciprocity method transforms the domain integral by a set of coordinate function $f^j(x)$:

$$\ddot{u}(x,t) \approx \sum_{j=1}^{N+L} f^j(x)\ddot{\alpha}^j(t) \ , \tag{6}$$

where the superimposed dot represents the time derivative, α^j are unknown functions of time, and N and L are the numbers of the boundary and selected internal nodes, respectively. In this study, the linear element is employed in the discretization and one internal point is placed in the

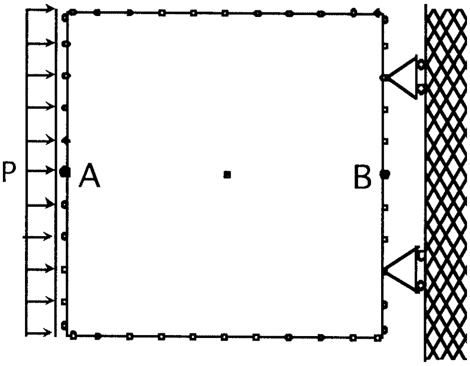

Fig. 1. BEM discretization of a square plate

center of domain. The resulting DRBEM formulation for this elastodynamic problem is given by

$$d_i u_i + \int_\Gamma (T^* u - u^* T) \mathrm{d}\Gamma = \sum_{j=1}^{N+L} \left[d_i \psi_i^j + \int_\Gamma \left(T^* \psi^j - u^* \eta^j \right) \mathrm{d}\Gamma \right] \left(\frac{\ddot{\alpha}^j}{\mu^2} + \lambda \dot{\alpha}^j \right) \ , \tag{7}$$

where $\eta^j = \partial \psi^j / \partial n$. Note that ψ^j is related to the specified coordinate functions $f^j(x)$ by

$$\nabla^2 \psi^j = f^j \ . \tag{8}$$

In the DRBEM, the radial basis function is often applied as functions $f^j(x)$. The efficiency and accuracy of the method depend greatly on choosing proper radial basis function. A detailed discussion of this topic is beyond the present study. For more related details see Agnantiaris et al. (1996), Golberg et al. (1998), Chen and Tanaka (2000), and the references therein. In the following numerical experiments, we use the linear radial basis function 1 + r in the dual reciprocity method (Nardini and Brebbia 1983; Partridge et al. 1992; Agnantiaris et al. 1996). The DRBEM formulation (7) is rewritten in matrix form as

$$M\ddot{u} + \mu^2 \lambda M \dot{u} + Hu - GT = 0 \ , \tag{9}$$

where M is the mass matrix comprised of the coordinate function column vectors, and H and G denote the whole matrices of boundary element with fundamental solution kernels T^* and u^*, respectively. Note that all coefficient matrices are dependent only on the geometric data. Since the displacement boundary conditions are involved in the tested problems, Eq. (9) is a differential algebraic system. By using a participation approach (Partridge et al. 1992), we can finally have

$$\ddot{u} + \mu^2 \lambda \dot{u} + ku = f \ , \tag{10}$$

where k represents stiffness matrix. The remaining solution procedure is the same as the treatment of the standard initial value problems. The desired traction can be easily calculated after the solutions of the above differential system are accomplished.

3 Time schemes

The details on the Houbolt and Newmark methods can be found in Bathe and Wilson (1976). Parameters $\alpha = 0.45$, $\delta = 0.72$ are taken in the damped Newmark method to increase the numerical damping. Due to the recent origins of the DQM and PIM, in the following we give a brief introduction to these two methods approximating time derivative.

3.1 DQM time approximation

The DQM analogue of the first derivative of function $f(t)$ is expressed as

$$\frac{\mathrm{d}f(t)}{\mathrm{d}t}\Big|_{t_i} = \sum_{j=1}^{N} A_{ij} f(t_j) \tag{11}$$

where t_j's are the discrete points in the temporal variable domain. $f(t_j)$ is the function values at these points, A_{ij} are the DQM weighting coefficients. By using simple algebraic transformation

$$z = u - u_0 - v_0 t + v_0 t_0 \ , \tag{12}$$

where t_0 is the initial instance of each DQM time element, and u_0 and v_0 are corresponding initial displacement and velocity, Eq. (10) is restated as

$$\ddot{z} + \mu^2 \lambda \dot{z} + kz = \bar{f} \ . \tag{13}$$

Note that the z and $\dot{z}$ at t_0 of each DQM time element are always zero due to the variable transformation of Eq. (12). The DQM analogue of the first-order time derivative can be rewritten as

$$\bar{A}\{z\} = \{\dot{z}\} \ , \tag{14a}$$

$$\bar{A}\{\dot{z}\} = \{\ddot{z}\} \ , \tag{14b}$$

where $\bar{A}$ is yielded by removing the first column of the original DQM weighting coefficient matrix A in Eq. (11). Substituting Eq. (14a) into Eq. (14b), we have

$$\overline{AA}\{z\} = \bar{B}\{z\} = \{\ddot{z}\} \ , \tag{15}$$

where $\bar{B}$ is the modified DQM coefficient matrix building into the two initial conditions. The above strategy exactly applying two initial conditions was originally presented by Chen (1996). In terms of approximate formulas (14a) and (15), Eq. (13) can be analogized as

$$Z\left(\bar{B}^T + \mu^2 \lambda \bar{A}^T\right) + KZ = F(t) \ , \tag{16}$$

It is noted that Z in Eq. (16) is a rectangular matrix rather than a vector. Therefore, Eq. (16) is a Lyapunov matrix equation. It is worth pointing out that the DQM discretization advances progressively in time domain element-wisely from the initial state, and thus keeps the simplicity and flexibility of the standard time step methods. On the other hand, the DQM also holds the unconditionally stable merit for accuracy of order more than two. This is due to the fact that the method is not a traditional time step scheme and circumvents the rigorous accuracy limitation for unconditionally stable algorithms due to Dahlquist theorem (Dahlquist 1963). The accuracy of the DQM is $O(\Delta t^{N-1})$ where N is the number of grid points in the DQM time element and Δt is time step size (Chen 1996).

Solving Eq. (16) by the LU decomposition method fails to fully utilize the special structure inherent with the Lyapunov equation so that the computing effort is not necessarily high. The Bartels–Stewart algorithm (Bartels and Stewart 1972) is a very efficient and stable technique to solve such Lyapunov algebraic matrix equation. The solution procedures include the following four steps:

Step 1: Reduce K and $\bar{B}^T + r^2 s \bar{A}^T$ of Eq. (16) into certain simple form via the similarity transformations $G = P^{-1}KP$ and $R = V^{-1}\left(\bar{B}^T + \mu^2 \lambda \bar{A}^T\right) V$.
Step 2: $Q = P^{-1}FV$ for the solution of Q.

Step 3: Solve the transformed equation $GY + YR = Q$ for Y.
Step 4: $Z = PYV^{-1}$.

The time-consuming calculation of $O(M^3)$ scalar multiplication is required only in step one for Eq. (16) of M dimension, while all implicit step methods also demand $O(M^3)$ operations. It is noted that operation in Step 1 needs to be done only once. On the other hand, Steps 2, 3 and 4 of the Bartels–Stewart algorithm need be executed repeatedly in each time element, which requires $O(M^2)$ multiplication. The standard step methods also demand analogous computational effort in each time step. Therefore, the total computing effort in the DQM is comparable to the common implicit step methods.

3.2
PIM time approximation

In the PIM, the DRBEM formulation (10) is at first reduced to the first-order problem

$$\dot{v} = Hv + r \ , \tag{17}$$

in which

$$v = \begin{Bmatrix} u \\ \dot{u} \end{Bmatrix}, \quad H = \begin{bmatrix} 0 & I \\ -k & -\mu^2\lambda \end{bmatrix}, \quad r = \begin{Bmatrix} 0 \\ 1 \end{Bmatrix} f(t) \ . \tag{18}$$

I is the unit matrix. The general solution v to Eq. (17) can be written as

$$v_{k+1} = T\left[v_k + H^{-1}\left(r_k + H^{-1}r_1\right)\right] - H^{-1}\left[r_{k+1} + H^{-1}r_1\right] \ , \tag{19}$$

where $r_1 = (r_{k+1} - r_k)/\tau$. τ is the time interval. Note that the loading has been assumed to vary linearly within time step $[t_k, t_{k+1}]$ in Eq. (19), i.e.,

$$r = r_k + r_1(t - t_k) \ . \tag{20}$$

T is given by

$$T = \exp(H\tau) \ . \tag{21}$$

The key step in the precise integration method is to evaluate the exponential matrix T accurately by

$$T(t) = [\exp(H\Delta\bar{t})]^m \ , \tag{22}$$

where $\Delta\bar{t} = \tau/m$, and $m = 2^N$. In this paper, $N = 20$ has been used to assure the accuracy of matrix T. Therefore, $\Delta\bar{t}$ is extremely small time interval and usually much less than the highest modal period of dynamic systems. By using a Taylor expansion, we have

$$\exp(H\Delta\bar{t}) \cong I + \left[H\Delta\bar{t} + (H\Delta\bar{t})^2/2! + (H\Delta\bar{t})^3/3! + (H\Delta\bar{t})^4/4!\right] = I + T_{a,0} \tag{23}$$

Substitution of Eq. (23) into Eq. (22) gives

$$T(t) = \left[I + T_{a,0}\right]^{2^N} \ . \tag{24}$$

A recurrence procedure of computing T was suggested (Zhong and Williams 1994; Lin et al. 1996):

$$T_{a,i} = 2T_{a,i-1} + T_{a,i-1} \times T_{a,i-1} \ . \tag{25}$$

Finally, we have

$$T = I + T_{a,N} \ . \tag{26}$$

The error in Eq. (26) is caused by the truncation of the Taylor expansion of Eq. (23). When $N = 20$, the truncation error is of the order $O(\Delta\bar{t}) = 10^{-30}O(\Delta\tau)$, which is of the order of the round-off errors of ordinary computers. So it is claimed that the T is obtained in the highest accuracy of a digital computer by the precise integration method (Zhong and Williams 1994; Lin et al. 1996).

4
Numerical results and discussions

In this study, the plates subjected to longitudinal half triangular, rectangular and Heaviside impact loads as shown in Fig. 2 are considered as the numerical examples. The initial conditions of the cases are taken as

$$u(x, 0) = 0 \ , \tag{27a}$$

$$\dot{u}(x, 0) = 0 \ , \tag{27b}$$

and boundary conditions are specified as

$$u(x, t) = 0, \quad x_1 = 1 \ , \tag{28a}$$

$$T(x, t) = 0, \quad x_1 = 0 \quad x_2 = 0, 1 \ . \tag{28b}$$

$\gamma = \lambda/\pi$ in the following discussions means the dimensionless damping coefficient. Mansur et al. (1998) also applied time domain BEM to accurately compute the Heaviside plate impact problems. We confine our attentions in this paper within the time integrators combined with the DRBEM. Thus, the discussions below do not involve the work of Mansur et al. (1998).

Figure 3 shows the solutions of time-displacement curves at middle point A of the free edge of the longitudinal vibration of a square plate subjected to a half-triangular impact force. Time step is $c\Delta t/t_0 = 0.1$. It is found from Fig. 3 that all methods yield the exact results using such sufficiently small time step. It is also noted that the PIM and DQM encounter small oscillation in the long-term response and their solutions are indistinguishable. On the other hand, the accurate solutions also reveal high degree of accuracy of the DRBEM spatial discretization. In order to manifest the high accuracy of the DQM and PIM in time approximation, we employed coarser time step $c\Delta t = 0.5$ to investigate the Heaviside impact time–displacement response at point A as shown in Fig. 4. The parameters $\alpha = 0.25$, $\delta = 0.5$ are taken in the Newmark method for this case. We observe quite distinct perfor-

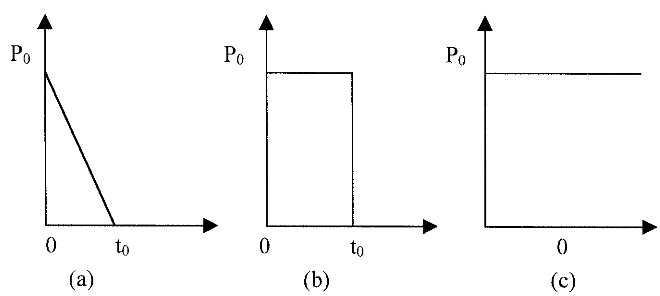

Fig. 2. Impact forces applied to plates

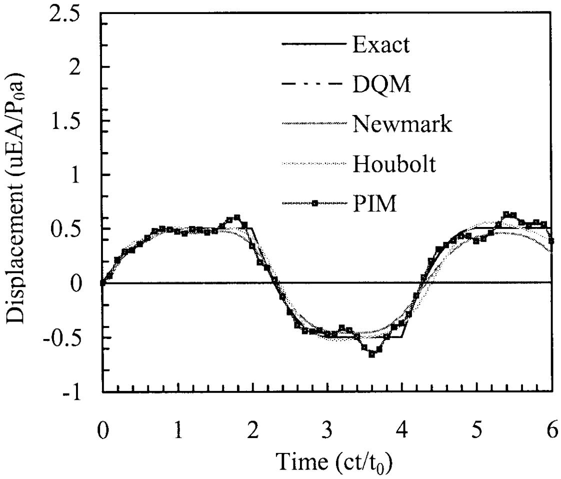

Fig. 3. Displacement curves at point A of a square plate subjected to a half-triangular impact ($\gamma = 0, c\Delta t/t_0 = 0.1$)

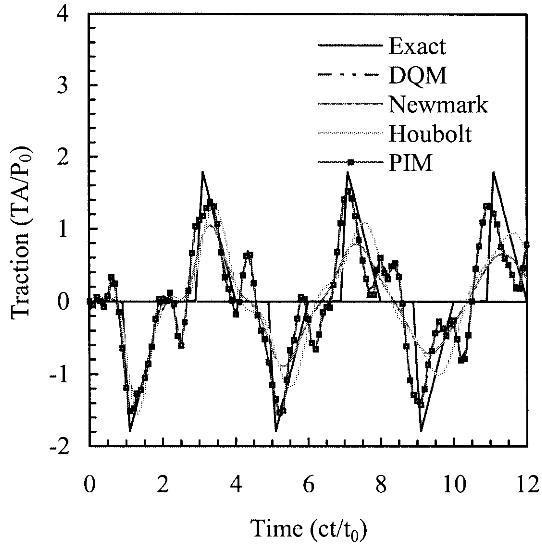

Fig. 5. Traction curves at point B of a square plate subjected half-triangular impact ($\gamma = 0, c\Delta t/t_0 = 0.1$)

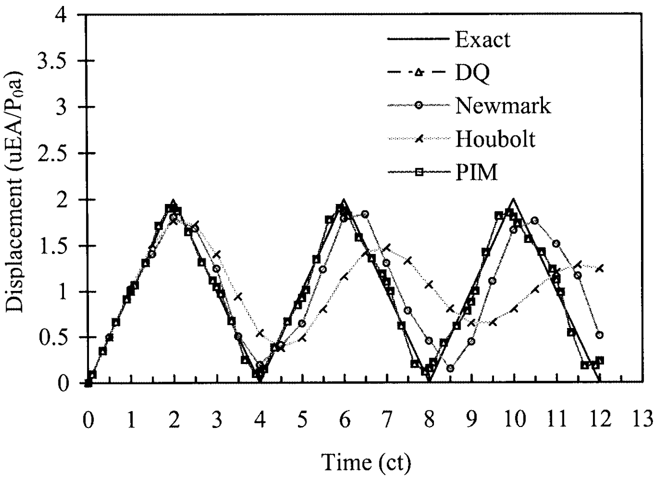

Fig. 4. Displacement curves at point A of a square plate subjected to a Heaviside-type impact ($\gamma = 0, c\Delta t = 0.5$)

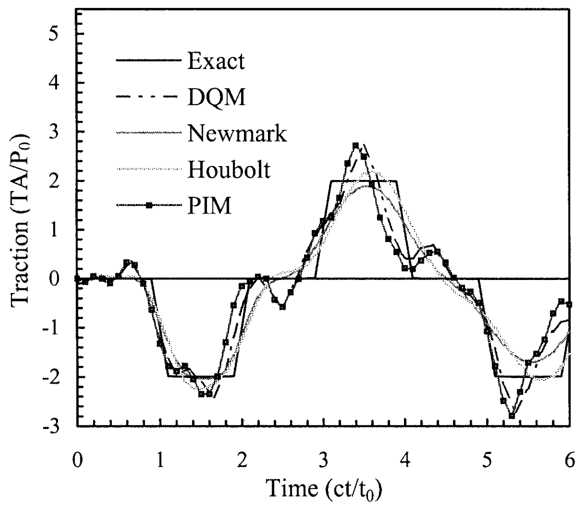

Fig. 6. Traction curves at point B of a square plate subjected to a rectangular impact ($\gamma = 0, c\Delta t/t_0 = 0.1$)

mances of various different time-marching schemes. The DQM and PIM produce much more accurate solutions than the standard finite difference integrators. This demonstrates the superb converging rate and accuracy of the DQM and PIM. In particular, the DQM requires computing resources comparable to the Newmark and Houbolt methods and much less than the PIM. Therefore, the DQM is preferred for this case. An evident amplitude attenuation and phase shift is observed in the Houbolt method due to its undesirable numerical damping in this case.

Figures 5 and 6 show the solutions of time–traction curves at point B of a square plate subjected to the half triangular and rectangular impact forces, respectively. The solutions of the DQM and PIM are found again almost the same and have evident oscillation. This is due to the fact that the high order models have strong effect on the traction behavior of the shock impact, while both methods lack artificial damping. It was seen from Figs. 5 and 6 that the solutions of the damped Newmark and Houbolt methods have less oscillations because of their high numerical damping. The DQM and PIM can not yield the exact traction response as in the previous displacement response where the lower and intermediate models dominate the response. The high artificial damping in the Newmark and Houbolt methods is considered beneficial in the present problems.

To investigate the influences of step size on the solutions of the traction responses, Figs. 7–10 depict the traction response curves using smaller time step $c\Delta t/t_0 = 0.05$. More evident oscillation can be found in the DQM and PIM solutions shown in Figs. 9 and 10, while the solution accuracy of the damped Newmark and Houbolt methods is improved as shown in Figs. 7 and 8. It is also found that the DQM and PIM yield nearly the same solutions.

Zhong and Williams (1994) and Lin et al. (1996) concluded that the PIM could produce the accurate solutions if the force function is approximated exactly. In the presented cases, the linear approximation of the half-trian-

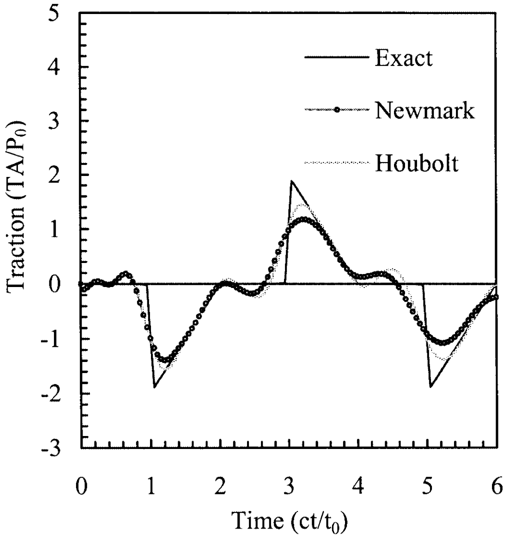

Fig. 7. Traction curves at point B of a square plate subjected to a half-triangular impact by the Newmark and Houbolt methods ($\gamma = 0, c\Delta t/t_0 = 0.05$)

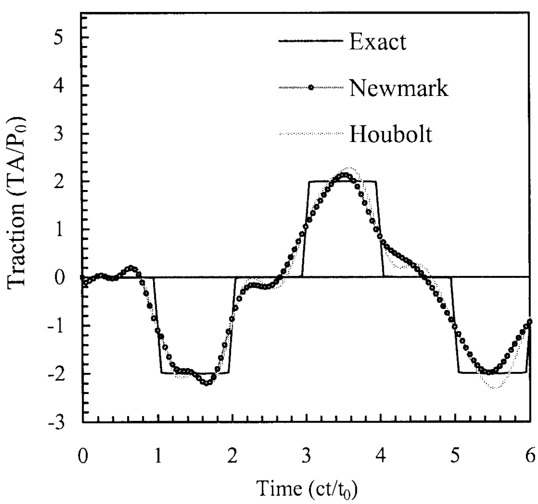

Fig. 8. Traction curves at point B of a square plate subjected to a rectangular impact by the Newmark and Houbolt methods ($\gamma = 0, c\Delta t/t_0 = 0.05$)

gular and rectangular impact force shown in Eq. (20) is exact. However, the PIM can not still traced the analytical solutions of traction response closely. To clarify whether the numerical oscillation in computing traction is due to the spatial approximation of the DRBEM, Figs. 11–14 illustrate the numerical traction response based on the DRBEM discretziation with 16 interior grid points in comparison with the previous one interior point.

The Newmark and Houbolt solutions of traction response using the DRBEM formulation of 16 interior points are displayed in Figs. 11 and 12 respectively for half triangular and rectangular impact forces. By comparing them with the corresponding solutions shown in Figs. 7 and 8, some improvements in solution accuracy are achieved due to the incremental interior points of the DRBEM spatial approximation. It is observed that the

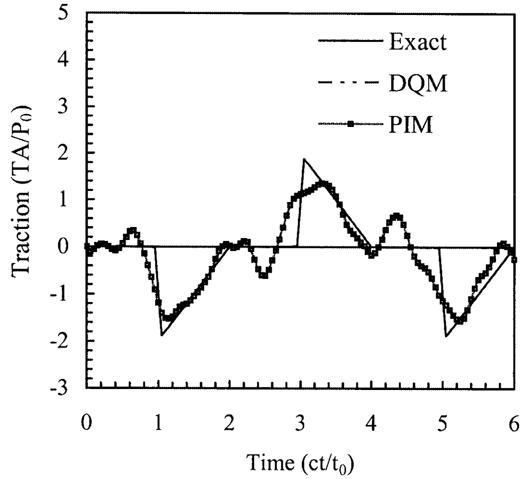

Fig. 9. Traction curves at point B of a square plate subjected to a half-triangular impact by the DQM and PIM ($\gamma = 0, c\Delta t/t_0 = 0.05$)

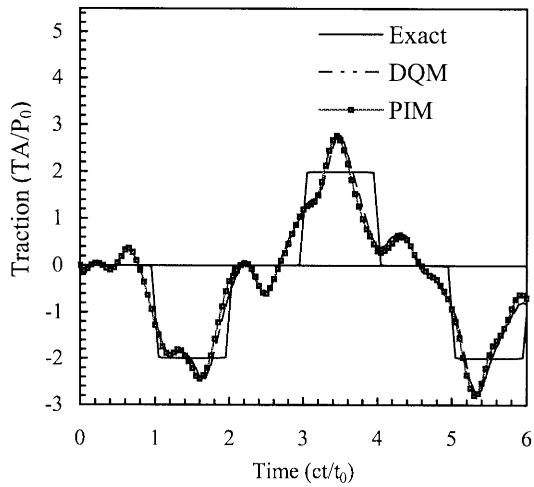

Fig. 10. Traction curves at point B of a square plate subjected to a rectangular impact by the DQM and PIM ($\gamma = 0, c\Delta t/t_0 = 0.05$)

Newmark method performs slightly better in rectangular impact force case, while the Houbolt method is more accurate in half-triangular impact force case. The present damped Newmark method appears to have higher numerical damping than the Houbolt method. It is worth pointing out that the damping of the Newmark method depends on two chosen parameters. Therefore, the Newmark method has more flexibility than the Houbolt method in practical computations.

Figures 13 and 14 show the traction response curves by the DQM and PIM in the context of the DRBEM spatial approximation using 16 interior points. It is surprise to see that the oscillation of the PIM and DQM becomes even stronger than the previous ones shown in Figs. 9 and 10 based on the one interior points DRBEM. Therefore, it is clear that the oscillation of the resulting solutions is mainly due to the numerical integrators rather than the DRBEM discretization itself. It is found again that the DQM and PIM yield the same traction response curves.

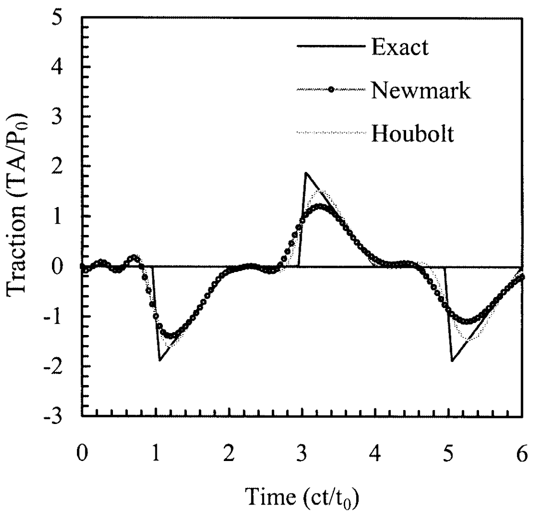

Fig. 11. Traction curves at point B of a square plate subjected to a half-triangular impact by the Newmark and Houbolt methods based on the DRBEM discretization with 16 interior points ($\gamma = 0, c\Delta t/t_0 = 0.05$)

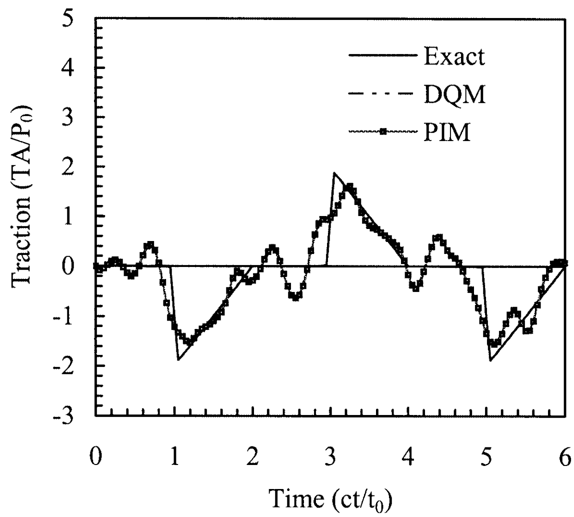

Fig. 13. Traction curves at point B of a square plate subjected to a half-triangular impact by the DQM and PIM based on the DRBEM discretization with 16 interior points ($\gamma = 0, c\Delta t/t_0 = 0.05$)

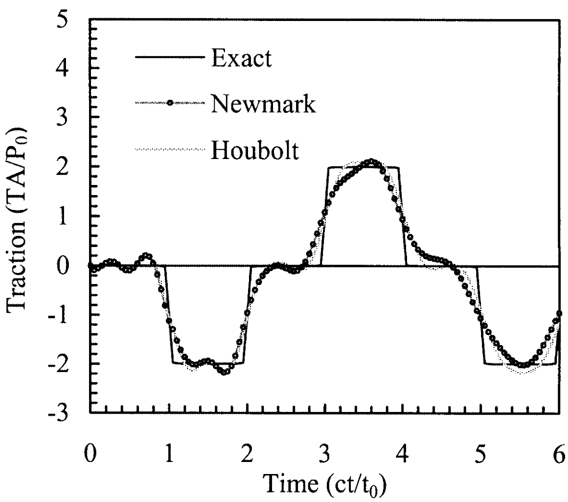

Fig. 12. Traction curves at point B of a square plate subjected to a rectangular impact by the Newmark and Houbolt methods based on the DRBEM discretization with 16 interior points ($\gamma = 0, c\Delta t/t_0 = 0.05$)

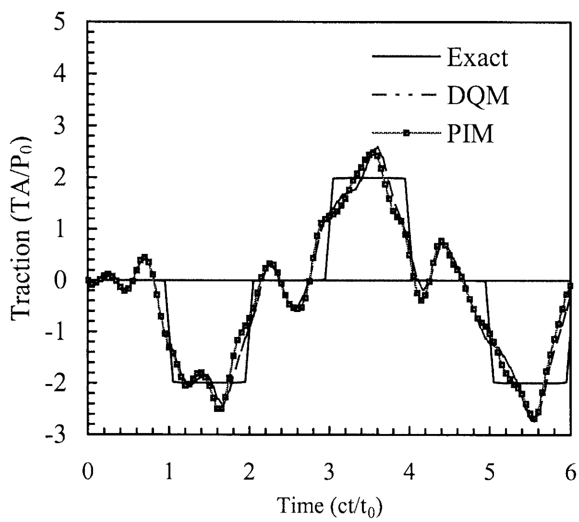

Fig. 14. Traction curves at point B of a square plate subjected to a rectangular impact by the DQM and PIM based on the DRBEM discretization with 16 interior points ($\gamma = 0, c\Delta t/t_0 = 0.05$)

The numerical experiments show that the accuracy is not a major factor in the choice of the numerical integrator for the analysis of impact traction response, especially if the very small time step is used.

The numerical response curves of traction at point B of a damped plate subjected to a Heaviside impact are depicted in Fig. 15 against the analytical solutions. High order frequency components have a strong affect on the traction behaviors of this case. It is seen from Fig. 15 that among the DQM, Houbolt and Newmark methods, the Houbolt and Newmark methods produce the accurate solutions, while the DQM encounters evident oscillation and phase shift due to the lack of artificial damping. It is also observed that the damped Newmark method yields slightly better solutions than the Houbolt method. Furthermore, considering the need of a distinct starting procedure in the Houbolt method, the method is not recommended.

5 Concluding remarks

It is noted that the DQM and PIM produce almost the same results for all tested cases. The resulting algebraic system of the DQM is found a Lyapunov matrix equation. By using the Bartels–Stewart solver, the DQM computational effort is greatly reduced to approximately the same as that of the common implicit step methods and much less than that of the PIM.

The preceding numerical experiments reveal that all these four numerical integrators can accurately compute the displacement responses of Heaviside, half-triangular

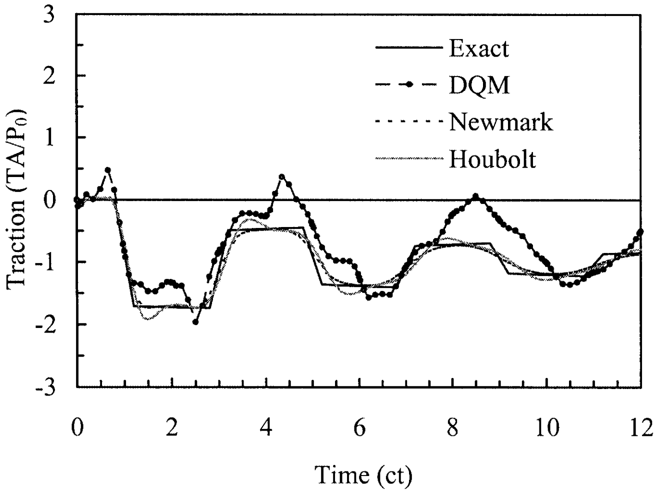

Fig. 15. Traction curves at point B of a square plate subjected to a Heaviside in-plane impact ($\gamma = 0.1, c\Delta t = 0.1$)

and rectangular impact forces. In terms of accuracy, efficiency and stability, the DQM is preferred to calculate impact displacement response, which is primarily dominated by low and intermediate frequency modes. However, there are quite distinct performances for impact traction responses since the higher modes play a significant role in this case. It is also found that the PIM and DQM always produce the oscillation solutions of traction response due to the absence of the numerical damping. In contrast, the high numerical damping in the damped Newmark and Houbolt methods is preferable.

For elastodynamic systems on which the high order modes have important effect, the numerical damping seems more important than the solution accuracy. Therefore, although the PIM and DQM enjoy the high order of accuracy than the Houbolt and Newmark methods, they are not recommended for handling traction analysis of the shock-excited vibration of elastodynamic bar. According to the foregoing numerical results, the damped Newmark method performs as well as the Houbolt method. Since the Newmark method does not need a distinct starting procedure, the method should be preferred in the combination with the DRBEM for analyzing this type of problems. This conclusion is in agreement with common practice in the FEM (Kim et al. 1997).

References

Agnantiaris JP, Polyzos D, Beskos DE (1996) Some studies on dual reciprocity BEM for elastodynamic analysis. Comput. Mech. 17(4): 270–277

Agnantiaris JP, Polyzos D, Beskos DE (1998) Three-dimensional structural vibration analysis by the dual reciprocity BEM. Comput. Mech. 21(4/5): 372–381

Bartels RH, Stewart GW (1972) A solution of the equation $AX + XB = C$. Commun. AM. 15: 820–826

Bathe K, Wilson EL (1976) Numerical Methods in Finite Element Analysis. Prentice-Hall, Englewood Cliffs, New Jersey

Bert CW, Malik M (1996) Differential quadrature method in computational mechanics: a review. Appl. Mech. Rev. 49: 1–28

Chen W (1996) Differential Quadrature Method and its Applications in Engineering-applying Special Matrix Product to Nonlinear Computations. Ph.D. Thesis. Shanghai Jiao Tong University

Chen W, Tanaka M (2000) New insights into boundary-only and domain-type RBF methods. Int. J. Nonlinear Sci. Numer. Simulation 1(3): 145–151

Dahlquist GA (1963) Special stability problem for linear multistep methods. BIT 3: 27–43

Golberg MA, Chen CS, Bowman H, Power H (1998) Some comments on the use of radial basis functions in the dual reciprocity method. Comput. Mech. 21: 141–148

Hilber HM, Hughes TJR (1978) Collocation, dissipation and 'overshoot' for time integration schemes in structural dynamics. Earthquake Eng. Struct. Dynamics 6: 99–117

Kim SJ, Cho JY, Kim WD (1997) From the trapezoidal rule to higher-order accurate and unconditionally stable time-integration method for structural dynamics. Comput. Meth. Appl. Mech. Eng. 149: 73–88

Kogl M, Gaul L (1999) Dual reciprocity boundary element method for three-dimensional problems of dynamic piezoelectricity. In: Proc. of Boundary Element XXI, WIT Press, Southampton, UK, pp. 537–548

Kontoni D, Beskos D (1993) Transient dynamic elastoplastic analysis by the dual reciprocity BEM. Eng. Anal. Boundary Elem. 12: 1–16

Lin J, Shen W, Williams FW (1996) A high precision direct integration scheme for structural subjected to transient dynamic loading. Comput. Struct. 38(1): 113–120

Loeffler CF, Mansur WJ (1987) Analysis of time integration schemes for boundary element applications to transient wave propagation problems. In: Proc. of BETECH'87, Comput. Mech. Publ., Southampton, UK

Mansur WJ, Carrer JAM, Siqueira EFN (1998) Time discontinuous linear traction approximation in time domain BEM scalar wave propagation analysis. Int. J. Numer. Meth. Eng. 42(2): 667–683

Nardini D, Brebbia CA (1983) A new approach to free vibration analysis using boundary elements. Appl. Math. Modeling 7: 157–162

Park KC (1975) An improved stiffly stable method for direct integration of nonlinear structural dynamic equations. ASME J. Appl. Mech. 42: 464–470

Partridge PW, Brebbia CA, Wrobel LW (1992) The Dual Reciprocity Boundary Element Method. Comput. Mech. Publ., Southampton, UK

Subbaraj K, Dokainish M (1989) A survey of direct time-integration methods in computational structural dynamics-II: implicit methods. Comput. Struct 32: 1387–1401

Tanaka M, Chen W (2001) Dual reciprocity BEM applied to transient elastodynamic problems with differential quadrature method in time. Comput. Meth. Appl. Mech. Eng. 190: 2331–2347

Tanaka M, Chen W (2001) Coupling dual reciprocity BEM and differential quadrature method for time-dependent diffusion problems. Appl. Math. Modeling 25: 257–268

Trujillo MD, Busby HR (1997) Practical Inverse Analysis in Engineering. CRC Press, New York

Zhong WX, Williams FW (1994) A precise time step integration method. J. Mech. Eng. Sci., Part C. 208(6): 427–430